

FIG. 2. Angular velocity components in the moving frame of reference. (1) *A* component, (2) *B* component, and (3) *C* component. *C* denotes "correlation function," as in all the following figures.

The moving frame of reference<sup>5</sup> is defined (as in part IV), by the equations

$$v_A = v_x e_{Ax} + v_y e_{Ay} + v_z e_{Az},$$

$$v_B = v_x e_{Bx} + v_y e_{By} + v_z e_{Bz},$$

$$v_C = v_x e_{Cx} + v_y e_{Cy} + v_z e_{Cz}.$$

In this notation  $e_A$ ,  $e_B$ , and  $e_C$  are unit vectors along the principal moment of inertia axes of the molecule.  $v_x$ ,  $v_y$ , and  $v_z$  are the components of  $\mathbf{v}$  in the laboratory frame and  $v_A$ ,  $v_B$ , and  $v_C$  are those in the moving frame. With these definitions the component correlation functions

$$\langle v_C(t)\omega_B(0) \rangle \text{ and } \langle v_B(t)\omega_C(0) \rangle,$$

exist for  $t > 0$ .

## RESULTS AND DISCUSSION

Figures 2–5 illustrate the effect of an increasing field strength on the moving frame components of the angular velocity correlation function. As the field strength increases the components become more oscillatory and more anisotropic in appearance.

In order to reproduce these effects analytically we

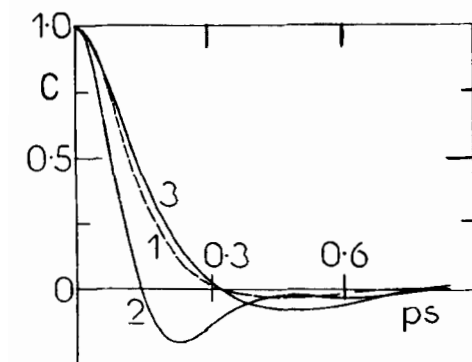


FIG. 3. Same as for Fig. 2, 8.75 *kT* field applied in the *Z* direction of the laboratory frame. The effect of this field is to increase the anisotropy of the angular motion, and all three components are oscillatory.

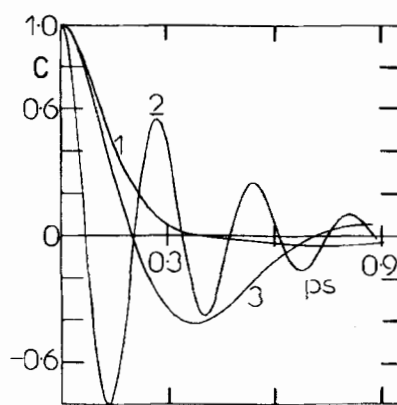


FIG. 4. Same as for Fig. 2, 17.5 *kT* field nearing the saturation level of the Langevin function. The *B* and *C* components of the angular velocity a. c. f. are now clearly oscillatory.

need to solve a Langevin or Kramers equation<sup>6</sup> structured so as to take into account: (a) an arbitrarily strong driving field<sup>7</sup>; (b) the effects of rotation-translation coupling<sup>4,5</sup>; and (c) the nonlinear interaction between a molecule and its surroundings.<sup>8–13</sup>

Grigolini *et al.*<sup>14</sup> have developed a formalism for dealing with the analytical problem associated with (a), as described in part IV of this series. The effects of rotation/translation coupling are illustrated in Figs. 6–9, in terms of  $\langle v_C(t)\omega_B(0) \rangle$  and  $\langle v_B(t)\omega_C(0) \rangle$ . These become more oscillatory again as the field strength increases to saturation level (equivalent to about 35 *kT*). The most interesting thing about these correlation functions is that they reveal features of *single molecule* diffusion which conventional theory does not commonly envisage let alone attempt to describe. In this respect the computer simulation method, with all its imperfections, is the only means of progress. It may be used to guide the theoretical analysis and interpret the

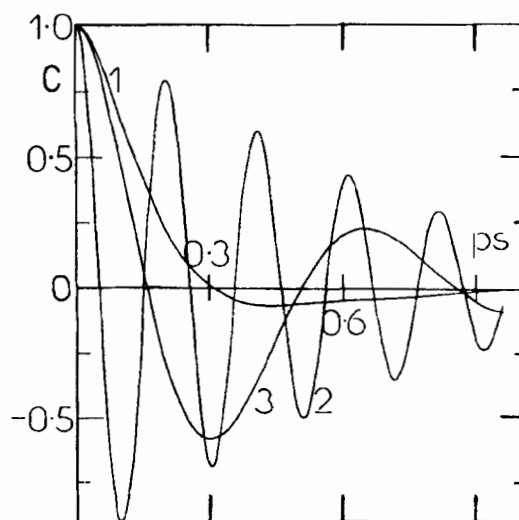


FIG. 5. Same as for Fig. 2, 35.0 *kT* field. The frequency of oscillation is clearly increased compared with Fig. 4.

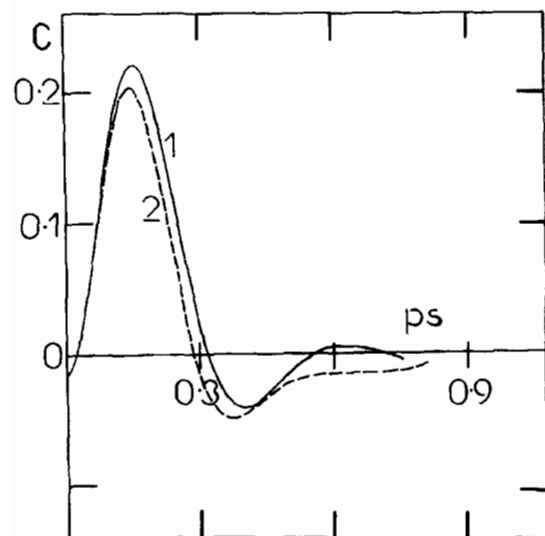


FIG. 6. (1)  $\langle v_C(t)\omega_B(0) \rangle / \langle v_C^2 \rangle^{1/2} \langle \omega_B^2 \rangle^{1/2}$ ; no field. (2) Same as for Fig. 1, 8.75 kT applied field.

experimental results. It is soon going to be possible to saturate the Langevin function for liquids such as  $\text{CH}_2\text{Cl}_2$  with megawatt power lasers, applied in picosecond pulses.

Essentially the problem facing the analytical theoretician is to rewrite the relevant equations in the moving frame of reference, solve these successfully for correlation functions such as  $\langle v_C(t)\omega_B(0) \rangle$ , etc., and then transform the results into the laboratory frame. In this frame  $\langle \mathbf{v}(t) \cdot \omega(0) \rangle$  or  $\langle \mathbf{v}(t)\omega(0)^T \rangle$  vanishes for all  $t$  and all strengths of applied field because of parity symmetry rules. (Note that these may not apply with magnetic fields or chiral molecules). The first attempt to carry out this procedure was made by Ferrario<sup>15</sup> with the rototranslational Langevin equations derived by Evans *et al.*<sup>16</sup> rewritten in the moving frame of reference. These Langevin type equations are single

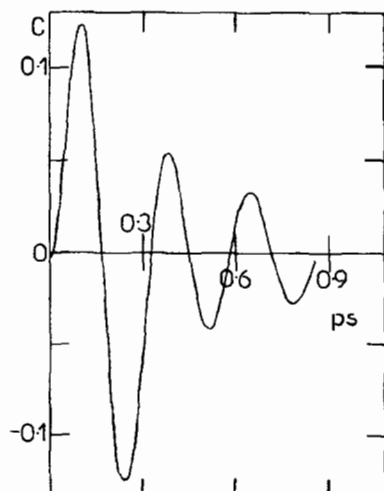


FIG. 7. (C, B) element, 17.5 kT applied field.

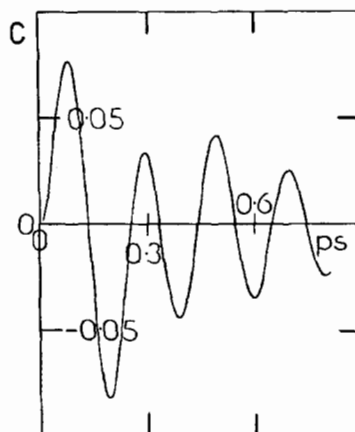


FIG. 8. Same as for Fig. 7, 35.0 kT applied field.

molecule in nature, the interaction with the environment being described by a combination of stochastic force/torque terms and rototranslational friction coefficients. They are insoluble analytically, but can be integrated numerically by stochastic simulation. When this is done, the moving frame correlation functions  $\langle v_C(t)\omega_B(0) \rangle$  and  $\langle v_B(t)\omega_C(0) \rangle$  are far too small in comparison with those of Figs. 6–9 and indeed do not rise above the abscissa on the ordinate scale of these diagrams.

Grigolini, Evans, Ferrario, and Marin<sup>17</sup> have traced the origin of this result to the neglect of nonlinear effects in the Langevin equation for single molecules. Specifically, the interaction between one molecule and its environment should depend on the details of the environment in quite specific ways. In other words, the details of the intermolecular potential must be built in to the traditional stochastic differential or integrodifferential equations. If we restrict our attention for the moment to center of mass linear velocity, a typical "nonlinear" system of equations would be<sup>17</sup>:

$$\begin{aligned} \dot{\mathbf{r}} &= \mathbf{v}, \\ \dot{\mathbf{v}} &= -\frac{\partial V}{\partial \mathbf{r}} - \zeta \mathbf{v} + \mathbf{F}(t), \end{aligned}$$

in the Markov limit. In this simplest of cases  $V$  the in-

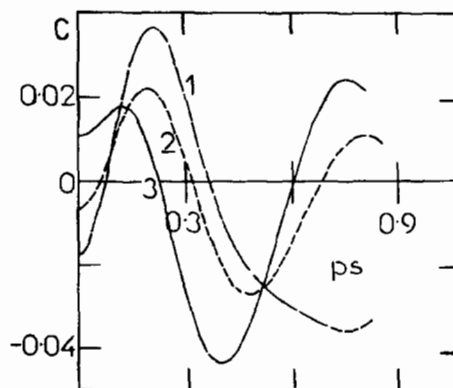


FIG. 9. Some  $\langle v_B(t)\omega_C(0) \rangle / \langle v_B^2 \rangle^{1/2} \langle \omega_C^2 \rangle^{1/2}$  elements; (1) 8.75 kT field, (2) 17.5 kT field; and (3) 35.0 kT field.

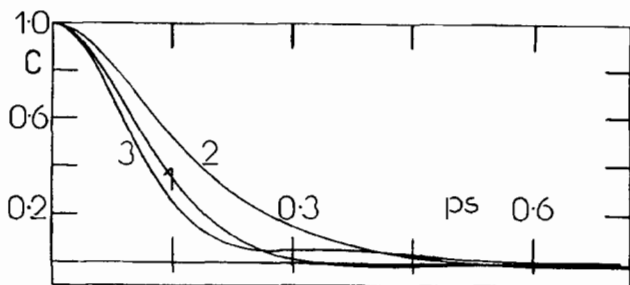


FIG. 10. (1), (2), and (3), respectively,  $\langle v_A(t)v_A(0) \rangle / \langle v_A^2 \rangle^{1/2}$ ;  $\langle v_B(t)v_B(0) \rangle / \langle v_B^2 \rangle^{1/2}$ ; and  $\langle v_C(t)v_C(0) \rangle / \langle v_C^2 \rangle^{1/2}$  in the moving frame of reference. Here  $V$  is the center of mass linear velocity. No applied field.

termolecular potential energy would have to be distance and angle dependent to attain a basic level of realism. [When we start adding to this basic analytical structure an external field term, and additionally attempt to describe the angular motion of the molecule, inertial and memory effects, the only means of obtaining a solution is either by stochastic simulation (i. e., numerical integration, making use of a random number generator), or by using (numerically) Dupuis renormalization algebra<sup>18</sup> on a long continued fraction of the Mori type, recently generalized by Grigolini *et al.*<sup>14</sup>] It is clear therefore that the computer simulation results provide an objective assessment of what is a profound analytical problem.

The components  $\langle v_A(t)v_A(0) \rangle$ ,  $\langle v_B(t)v_B(0) \rangle$ , and  $\langle v_C(t)v_C(0) \rangle$  are illustrated in Figs. 10 and 11. The effect of the applied torque  $\mathbf{e}_A \times \mathbf{E}$  is clearly transmitted to the center of mass movement through functions such as those in Figs. 6–9. These components are not identical in the moving frame.

One of the interesting side effects of a nonlinear theory of molecular diffusion is its ability, recently demonstrated by Grigolini *et al.*,<sup>19</sup> to produce non-Gaussian behavior in the transient region (between  $t = 0$  and equilibrium) of certain correlation functions. Switching our attention to the laboratory frame, the transiently non-Gaussian nature of the velocity autocorrelation function  $\langle \mathbf{v}(t) \cdot \mathbf{v}(0) \rangle$  is illustrated in Fig. 12 using the method developed by Berne and Harp.<sup>20</sup> Note that the computer simulation accurately produces the Gaussian equilibrium level of  $3/5$  in  $\langle v^2(t)v^2(0) \rangle / \langle v^4(0) \rangle$

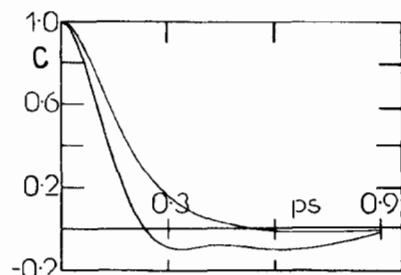


FIG. 11. Top:  $B$  component; bottom:  $A$  component of the moving-frame velocity a. c. f.,  $35.0 \text{ kT}$  applied field.

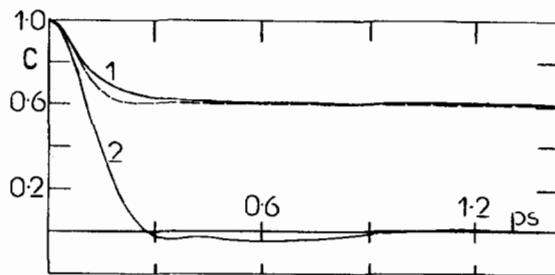


FIG. 12. The non-Gaussian nature of the velocity autocorrelation function  $\langle \mathbf{v}(t) \cdot \mathbf{v}(0) \rangle$  in the laboratory frame.  $35.0 \text{ kT}$  applied field. (1)  $\langle v^2(t)v^2(0) \rangle / \langle v^4(0) \rangle$ , (2)  $\langle \mathbf{v}(t) \cdot \mathbf{v}(0) \rangle / \langle v^2(0) \rangle$ ,  $--- \frac{3}{5} [1 + \frac{3}{5} \langle \mathbf{v}(t) \cdot \mathbf{v}(0) \rangle / \langle v^2(0) \rangle]^2$ , the Gaussian result.

even in the presence of a very strong field (equivalent in energy to  $35 \text{ kT}$ ). The analytical theory should obviously aim to reproduce the solid upper line in Fig. 12 rather than the dashed line.

The angular velocity correlation function in the laboratory frame  $\langle \omega(t) \cdot \omega(0) \rangle / \langle \omega^2(0) \rangle$ , and the angular kinetic energy a. c. f.  $\langle \omega^2(t)\omega^2(0) \rangle / \langle \omega^4(0) \rangle$  are illustrated in Fig. 13 under an applied field equivalent energetically to  $35 \text{ kT}$ . For comparison, the Gaussian result<sup>19</sup> is also plotted, and the transient statistics are clearly not Gaussian.

Finally, in Fig. 14 we plot the  $35 \text{ kT}$  mixed correlation function

$$\frac{\langle v^2(t)\omega^2(0) \rangle}{\langle v^2(0) \rangle \langle \omega^2(0) \rangle}$$

For Gaussian statistics this is one for all  $t$ , and this is yet another clear demonstration of the need to improve currently available analytical theory.

### SATURATING THE LANGEVIN FUNCTION: THE FAR INFRARED

The far infrared is the frequency region equivalent to picoseconds on the time scale of molecular dynamics. In the simplest term the Poley absorption of dipolar liquids is the Fourier transform of, in our notation  $\langle \dot{\mathbf{e}}_A(t) \cdot \dot{\mathbf{e}}_A(0) \rangle$ , the rotational velocity correlation function

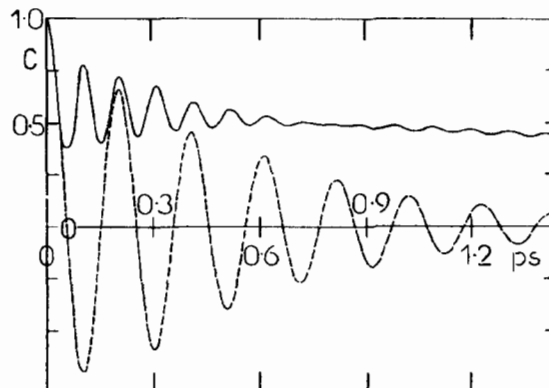


FIG. 13. Same as for Fig. 12, angular velocity  $\omega$  laboratory frame of reference.

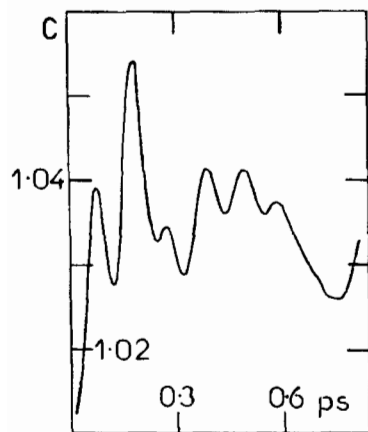


FIG. 14. The mixed second-moment a. c. f. :  $\langle v^2(t)\omega^2(0) \rangle / \langle v^2 \rangle \langle \omega^2 \rangle$ , 35.0 kT applied field. For Gaussian statistics this remains at one for all  $t$ .

of the dipole unit vector  $\mathbf{e}_A$ . This c. f. is illustrated in Fig. 15 for a 35 kT field and for the field-off case. In the field-on case  $\langle \mathbf{e}_A(t) \cdot \mathbf{e}_A(0) \rangle$  and  $\langle \omega(t) \cdot \omega(0) \rangle$  (Fig. 16) are almost identical. This comes from the kinematic relation

$$\dot{\mathbf{e}}_A = \boldsymbol{\omega} \times \mathbf{e}_A$$

and from the fact that one component of  $\langle \mathbf{e}_A(t) \cdot \mathbf{e}_A(0) \rangle$  falls to an equilibrium level of only 0.95 [Fig. 1(b)] instead of the field-off level of 0.

It is abundantly clear from Fig. 15 that the effect of the 35 kT field is to shift the far infrared Poley peak absorption<sup>8</sup> to a higher frequency and to sharpen it very considerably. This observation provides us with a sensitive method of studying molecular dynamics at Langevin saturation by monitoring the effect of a powerful (MW) laser on far infrared spectrum of  $\text{CH}_2\text{Cl}_2$ . This experiment is planned with the Atomic and Molecular Physics Institute of the CNR at Pisa, Italy, with Salvetti *et al.*

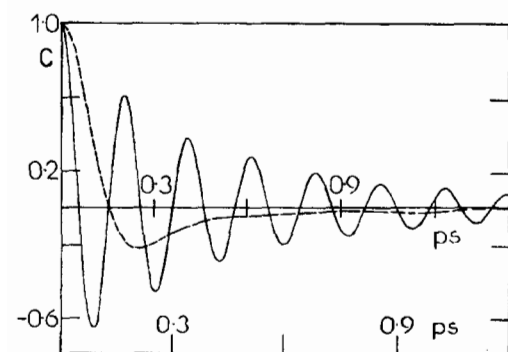


FIG. 15. — Rotational velocity autocorrelation function:  $\langle \dot{\mathbf{e}}_A(t) \cdot \dot{\mathbf{e}}_A(0) \rangle / \langle \dot{\mathbf{e}}_A^2(0) \rangle$ , 35 kT field of the dipole unit vector  $\lambda \mathbf{e}_A$ . The oscillatory structure of this function means that the far infrared peak is sharpened and shifted to high frequencies in comparison with the field off case. --- No field applied (lower abscissa scale).

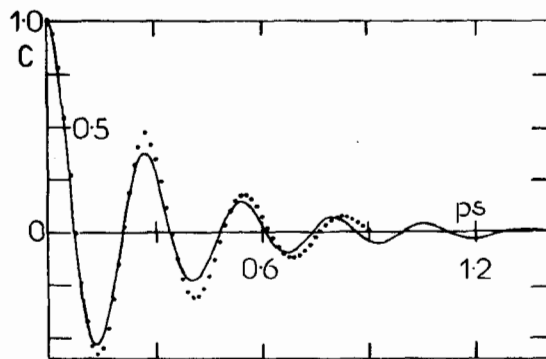


FIG. 16. Comparison of the — rotational velocity and  $\circ$  angular velocity a. c. f. at 17.5 kT applied field.

### SATURATING THE LANGEVIN FUNCTION: DIELECTRIC RELAXATION

The problem of how a dielectric loss spectrum responds to a perturbation greater than  $kT$  in energy has been treated by Ullman.<sup>21</sup> According to this author, the loss curve is shifted to higher frequencies by the application of the field. However, in the normal course of events, the dielectric relaxation time naturally lengthens as the barrier to diffusion increases.<sup>6</sup> Relaxation times about the long axis in a mesophase are, e.g., much longer than those in the isotropic phase of the same molecule at roughly similar temperatures. At the same time, the liquid in the presence of an aligning field greater than  $kT$  (in energetic terms) is of course birefringent, so that components of the dipole a. c. f.  $\langle \mathbf{e}_A(t) \cdot \mathbf{e}_A(0) \rangle$  behave differently.

By reference to computer simulation results such as those in Fig. 17, it is clear that the effect of the field is to decrease the correlation time along the laboratory  $Z$  axis (the field direction). To establish these results using stochastic differential equations would be a difficult

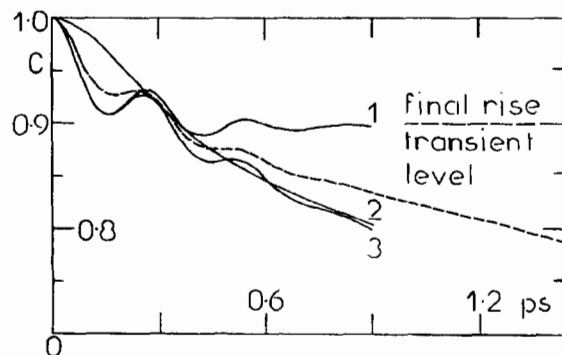


FIG. 17. The effect of a 17.5 kT field on the orientational a. c. f.  $\langle \mathbf{e}_A(t) \cdot \mathbf{e}_A(0) \rangle$  (observable in dielectric spectroscopy), dotted line. The laboratory frame components of this a. c. f. are marked 1, 2, and 3, and one goes to a final level of about 0.90. This point is also marked on Fig. 1(b) is the graph of  $\langle e_{AZ}^2 \rangle$  vs energy ratio—the Langevin function. The other two components go to zero, so that the complete a. c. f.  $\langle \mathbf{e}_A(t) \cdot \mathbf{e}_A(0) \rangle$  goes to about  $3/5$  as  $t \rightarrow \infty$ . The  $1/e$  correlation time in the absence of the field is 0.5 ps, and shorter in the presence of the field. The latter refers to the c. t. of  $\langle \mathbf{e}_A(t) \cdot \mathbf{e}_A(0) \rangle - \langle e_{AZ}^2 \rangle$ .

task, and they are, at the same time, valuable for the interpretation of laser-induced birefringence.

## CONCLUSIONS

(1) The computer simulation method has been used to investigate the molecular dynamics of  $C_{2v}$  symmetry asymmetric tops at points along the Langevin function to saturation.

(2) The first-order correlation function between molecular linear velocity  $\mathbf{v}$ , and angular velocity  $\omega$  is visible in a moving frame of reference and becomes oscillatory at high field strengths.

(3) In order to explain the numerical indications, a theory of rotational diffusion is required which details the intermolecular interaction more accurately than up to now. The simple concepts behind the Langevin equation, even when modified for moving-frame rototranslation, no longer work.

(4) The computer results, even at  $35 kT$ , are accurately Gaussian at equilibrium, but are transiently non-Gaussian.

(5) The computer simulation may be used to predict the results of experiments in laser-induced birefringence.

## ACKNOWLEDGMENT

The SERC is acknowledged for financial support.

## APPENDIX

In this appendix we note the Gaussian relation between the first and second moments of the angular velocity autocorrelation function. Following Ferrario's derivation we have<sup>19</sup>

$$\langle \omega(0) \cdot \omega(0) \omega(0) \cdot \omega(0) \rangle = 3 \left( \frac{kT}{I_1} \right)^2 + 3 \left( \frac{kT}{I_2} \right)^2 + 3 \left( \frac{kT}{I_3} \right)^2 + 2(kT)^2 \left( \frac{1}{I_1 I_2} + \frac{1}{I_2 I_3} + \frac{1}{I_3 I_1} \right),$$

$$\langle \omega(t) \cdot \omega(t) \omega(0) \cdot \omega(0) \rangle = (kT)^2 \left[ \left( \frac{1}{I_1} + \frac{1}{I_2} + \frac{1}{I_3} \right)^2 + \frac{2\chi_1^2}{I_1^2}(t) + \frac{2\chi_2^2}{I_2^2}(t) + \frac{2\chi_3^2}{I_3^2}(t) \right],$$

where

$$\chi_1(t) = \langle \omega_1(t) \omega_1(0) \rangle / \langle \omega_1(0) \omega_1(0) \rangle,$$

$$\chi_2(t) = \langle \omega_2(t) \omega_2(0) \rangle / \langle \omega_2(0) \omega_2(0) \rangle,$$

$$\chi_3(t) = \langle \omega_3(t) \omega_3(0) \rangle / \langle \omega_3(0) \omega_3(0) \rangle,$$

are the *moving frame* components of the angular velocity a. c. f. This frame is defined by the axes of  $I_1$ ,  $I_2$ , and  $I_3$  the principal moments of inertia. These equations have been used to calculate the Gaussian curve in Fig. 13.

<sup>1</sup>M. W. Evans, J. Chem. Phys. **76**, 5473 (1982).

<sup>2</sup>M. W. Evans, J. Chem. Phys. **76**, 5480 (1982).

<sup>3</sup>M. W. Evans, J. Chem. Phys. **77**, 4632 (1982).

<sup>4</sup>M. W. Evans, J. Chem. Phys. (in press, 1982).

<sup>5</sup>J.-P. Ryckaert, A. Belleman, and G. Ciccotti, Mol. Phys. **44**, 979 (1981).

<sup>6</sup>M. W. Evans, G. J. Evans, W. T. Coffey, and P. Grigolini, *Molecular Dynamics* (Wiley-Interscience, New York, 1982).

<sup>7</sup>M. W. Evans, M. Ferrario, and P. Grigolini, J. Chem. Soc. Faraday Trans. 2 **76**, 542 (1980).

<sup>8</sup>H. Risken and H. D. Vollmer, Z. Phys. Chem. Abt. B **31**, 209 (1978).

<sup>9</sup>E. Praestgaard and N. G. van Kampen, Mol. Phys. **43**, 33 (1981).

<sup>10</sup>M. W. Evans, M. Ferrario, and W. T. Coffey, Adv. Mol. Rel. Int. Proc. **20**, 1 (1981).

<sup>11</sup>P. Grigolini, M. Giordano, and P. Marin, Chem. Phys. Lett. **83**, 554 (1981).

<sup>12</sup>P. Grigolini, presented at the 6th S. P. C. Conference, Taormina, Sicily, 1981.

<sup>13</sup>A. Morita, J. Phys. A Math. Nucl. Gen. **12**, 991 (1979).

<sup>14</sup>P. Grigolini, M. Ferrario, and M. W. Evans, Physica A (in press).

<sup>15</sup>M. W. Evans and M. Ferrario, Chem. Phys. (in press).

<sup>16</sup>M. W. Evans, P. Grigolini, and M. Ferrario, Mol. Phys. **39**, 1369, 1391 (1980).

<sup>17</sup>P. Grigolini, M. W. Evans, M. Ferrario, and P. Marin, J. Chem. Phys. (in press).

<sup>18</sup>M. Dupuis, Prog. Theor. Phys. **37**, 502 (1967).

<sup>19</sup>P. Grigolini, M. Ferrario, and M. W. Evans, Z. Phys. Chem. Abt. B **41**, 165 (1981).

<sup>20</sup>B. J. Berne and G. D. Harp, Adv. Chem. Phys. **17**, (1970).

<sup>21</sup>R. Ullman, J. Chem. Phys. **69**, 1869 (1972).